

ORIGINAL RESEARCH

Treatment response of colorectal cancer liver metastases to neoadjuvant or conversion therapy: a prospective multicentre follow-up study using MRI, diffusion-weighted imaging and ¹H-MR spectroscopy compared with histology (subgroup in the RAXO trial)

A. Uutela¹, A. Ovissi^{2†}, A. Hakkarainen^{2,3‡}, A. Ristimäki⁴, N. Lundbom², R. Kallio⁵, L. M. Soveri⁶, T. Salminen⁷, A. Ålgars⁸, P. Halonen⁹, R. Ristamäki⁸, A. Nordin¹, R. Blanco Sequeiros^{10,11}, I. Rinta-Kiikka^{12,13}, E. Lantto¹⁴, J. Virtanen¹⁰, E. Pääkkö¹¹, E. Liukkonen¹¹, J. Saunavaara¹⁰, P. Ryymin^{12,13}, E. Lammintausta¹¹, P. Osterlund^{7,9,15*§} & H. Isoniemi^{1§},
on behalf of the RAXO Study Group[†]

¹Department of Transplantation and Liver Surgery, Helsinki University Hospital and University of Helsinki, Helsinki; ²Department of Radiology, HUS Medical Imaging Centre, Helsinki University Hospital and University of Helsinki, Helsinki; ³Department of Neuroscience and Biomedical Engineering, Aalto University School of Science, Helsinki; ⁴Department of Pathology, HUS Diagnostic Centre and Applied Tumour Genomics, Research Programs Unit, Helsinki University Hospital and University of Helsinki, Helsinki; ⁵Department of Oncology, Oulu University Hospital, Oulu; ⁶Joint Municipal Authority for Health Care and Social Services in Keski-Uusimaa, Home Care Geriatric Clinic and Palliative Care, Hyvinkää; ⁷Department of Oncology, Tampere University Hospital and University of Tampere, Tampere; ⁸Department of Oncology, Turku University Hospital and University of Turku, Turku; ⁹Department of Oncology, Helsinki University Hospital Comprehensive Cancer Center and University of Helsinki, Helsinki; ¹⁰Department of Radiology, Turku University Hospital and University of Turku, Turku; ¹¹Department of Radiology, Oulu University Hospital, Oulu; Departments of ¹²Radiology; ¹³Medical Physics, Medical Imaging Centre Tampere University Hospital and University of Tampere, Tampere; ¹⁴Department of Radiology, Päijät-Häme Central Hospital, Lahti, Finland; ¹⁵Department of Pathology/Oncology, Karolinska Institutet and Karolinska sjukhuset - Tema Cancer, Stockholm, Sweden



Available online 26 July 2021

Background: Colorectal cancer liver metastases respond to chemotherapy and targeted agents not only by shrinking, but also by morphologic and metabolic changes. The aim of this study was to evaluate the value of advanced magnetic resonance imaging (MRI) methods in predicting treatment response and survival.

Patients and methods: We investigated contrast-enhanced MRI, apparent diffusion coefficient (ADC) in diffusion-weighted imaging and ¹H-magnetic resonance spectroscopy (¹H-MRS) in detecting early morphologic and metabolic changes in borderline or resectable liver metastases, as a response to first-line neoadjuvant or conversion therapy in a prospective substudy of the RAXO trial (NCT01531621, EudraCT2011-003158-24). MRI findings were compared with histology of resected liver metastases and Kaplan–Meier estimates of overall survival (OS).

Results: In 2012–2018, 52 patients at four Finnish university hospitals were recruited. Forty-seven patients received neoadjuvant or conversion chemotherapy and 40 liver resections were carried out. Low ADC values (below median) of the representative liver metastases, at baseline and after systemic therapy, were associated with partial response according to RECIST criteria, but not with morphologic MRI changes or histology. Decreasing ADC values following systemic therapy were associated with improved OS compared to unchanged or increasing ADC, both in the liver resected subgroup (5-year OS rate 100% and 34%, respectively, $P = 0.022$) and systemic therapy subgroup (5-year OS rate 62% and 23%, $P = 0.049$). ¹H-MRS revealed steatohepatosis induced by systemic therapy.

Conclusions: Low ADC values at baseline or during systemic therapy were associated with treatment response by RECIST but not with histology, morphologic or detectable metabolic changes. A decreasing ADC during systemic therapy is associated with improved OS both in all patients receiving systemic therapy and in the resected subgroup.

Key words: colorectal cancer, liver metastasis, neoadjuvant chemotherapy, liver surgery, diffusion-weighted imaging, magnetic resonance spectroscopy

*Correspondence to: Prof. Pia Osterlund, Department of Oncology, Tampere University Hospital and University of Tampere, Teiskontie 35, 33520 Tampere, Finland; or Department of Oncology/Pathology at Karolinska Institutet, Karolinska Comprehensive Cancer Center, Eugeniavägen 3, 17164 Solna, Sweden.
Tel: +358-50-3375000 or +46-72-4694817

E-mail: pia.osterlund@helsinki.fi (P. Osterlund).

† Members are listed in the Acknowledgements.

‡ These authors share equal second authorship.

§ These authors share equal last authorship.

2059-7029/© 2021 The Authors. Published by Elsevier Ltd on behalf of European Society for Medical Oncology. This is an open access article under the CC BY license (<http://creativecommons.org/licenses/by/4.0/>).

INTRODUCTION

Liver is the most common metastatic location in metastatic colorectal cancer (mCRC), seen in 68%–71% when metastatic disease is diagnosed.^{1,2} Without metastasectomy, the prognosis of mCRC is poor. The reported 5-year overall survival (OS) rate after resection ranges between 32% and 50% in population-based studies.^{1,3} Liver metastases can initially be considered resectable in up to 20% of patients,⁴

and a further 22% may be converted resectable with effective systemic therapy.⁵ Systemic therapy is based on fluoropyrimidines combined with oxaliplatin and/or irinotecan. The addition of targeted agents further improves response rates and thus conversion rates. Vascular endothelial growth factor (VEGF) antibodies, e.g. bevacizumab, or epidermal growth factor receptor (EGFR) antibodies, e.g. cetuximab or panitumumab, are commonly used.⁶⁻⁸

The treatment of mCRC is multidisciplinary and a key element is detailed anatomic imaging to determine metastatic spread and resectability.⁹ Contrast-enhanced (CE) computed tomography (CT) and magnetic resonance imaging (MRI) are the most widely used imaging tools for preoperative planning in liver surgery. The high soft tissue contrast makes MRI a valuable tool in the characterisation and response evaluation of liver lesions, especially for lesions smaller than 10 mm and even more so in the presence of hepatic steatosis.¹⁰ Modern MRI techniques combine anatomic and metabolic information of metastases and liver parenchyma. Diffusion-weighted imaging (DWI) describes the microscopic movement of water molecules, which is more limited in tissues with high cell density, intact cell membranes and viscous fluid.^{11,12} This limited movement leads to high signal on high b-value DWI and low diffusion values on apparent diffusion coefficient (ADC) maps. The ADC correlates inversely to cell density. Changes in tumour cellularity can be detected using DWI and ADC values, and this could be a tool in clinical decision making.¹³

RECIST 1.1 criteria, the gold standard of treatment response evaluation, are based on tumour shrinkage.^{14,15} The VEGF antibodies cause tumour necrosis by disrupting the pathologic vascular network of the tumour. This will eventually lead to reduction in tumour diameter, but could be detected earlier and more accurately by changes in tumour appearance and metabolic activity.¹⁶⁻¹⁹ Morphologic response criteria for CT imaging have been proposed to detect these responses,¹⁶ but to our knowledge, no corresponding criteria have been applied for MRI.

Hepatic steatosis can to some extent be evaluated with routine preoperative CT and MRI sequences, but a more detailed tissue characterisation needs special techniques.²⁰ ¹H-magnetic resonance spectroscopy (¹H-MRS) is a non-invasive technique for analysing tissue metabolism and chemical composition, where results are often expressed using choline ratio to other metabolites. A ¹H-MRS examination can readily be combined with a normal diagnostic liver MRI.

In this prospective study, gadolinium CE-MRI, DWI and ¹H-MRS were used to assess treatment response of liver metastases, and compared with RECIST response, morphologic MRI response criteria, histopathological findings and survival. A secondary aim was to assess ¹H-MRS in evaluation of liver steatosis and chemotherapy-induced liver injury.

PATIENTS AND METHODS

Study design

The present study is a pre-planned substudy in the prospective nationwide investigator-initiated RAXO study in

Finland (NCT01531621, EudraCT2011-003158-24).^{21,22} In this substudy, inclusion was between December 2012 and September 2018. The protocol (Supplementary Material, available at <https://doi.org/10.1016/j.esmooop.2021.100208>) was approved by the Ethics Committee at Helsinki University Hospital. The study was conducted in accordance with the Good Clinical Practice and Declaration of Helsinki and monitored independently.

Patients

The patients were recruited at 4 university hospitals, out of 21 hospitals participating in the study. The inclusion criteria were histologically confirmed CRC with liver-limited metastases, scheduled for first-line oncologic treatment and age over 18 years. A thoraco-abdominopelvic CT was used to detect the metastases before inclusion. All patients provided written informed consent. The oncologist, radiologist and physicist identified patients before first appointment at oncology, as MRI was to be carried out after consent to substudy at first visit and before treatment initiation. The protocol included a baseline MRI, which was repeated after 8-12 weeks of systemic therapy. The study flow chart is shown in Supplementary Figure S1, available at <https://doi.org/10.1016/j.esmooop.2021.100208>. The data cut-off date for follow-up was 4 May 2020.

Liver MRI protocol

MR examinations were carried out with three Tesla Siemens Verio or Skyra (Siemens Healthineers, Erlangen, Germany) imagers. At least T2-/T1-weighted, in-phase/out-phase, DWI sequences and ¹H-MRS of the largest or most appropriate metastasis, and in normal-appearing liver, and dynamic images with gadolinium contrast agent CE-MRI were acquired. All the contrast-free sequences were done before injecting the contrast agent. As the heart pulsation may cause artefact especially in the ¹H-MRS of the left liver lobe, a suitable patient should have an at least 2-cm metastasis in the right liver lobe. In DWI acquisition, a stack of transaxial images, with a slice thickness of 5-6 mm, covering the whole liver was collected applying single-shot echo-planar imaging DWI incorporated with three orthogonal diffusion gradient directions sequentially using three different b-values of 100, 400 and 800 s/mm². The DWI series was obtained before ¹H-MRS and was utilised in voxel placement for the subsequent ¹H-MRS. Firstly, a cubic 2 × 2 × 2-cm³ MRS voxel was placed in normal-appearing liver parenchyma avoiding lesions and large vascular structures. Secondly, a lesion spectrum was placed in the active tumour area of the largest metastasis avoiding areas appearing necrotic typically in the centre of the large metastases. Point-resolved spectroscopy technique was used for spatial localisation to obtain spectra with an echo time of 30 ms and repetition times of >4000 ms and >8000 ms, for liver parenchyma and lesion spectra, respectively. Two and sixteen signals were averaged for unsuppressed and water-suppressed spectra, respectively. The total duration of this MRI protocol was about 1 h, which is

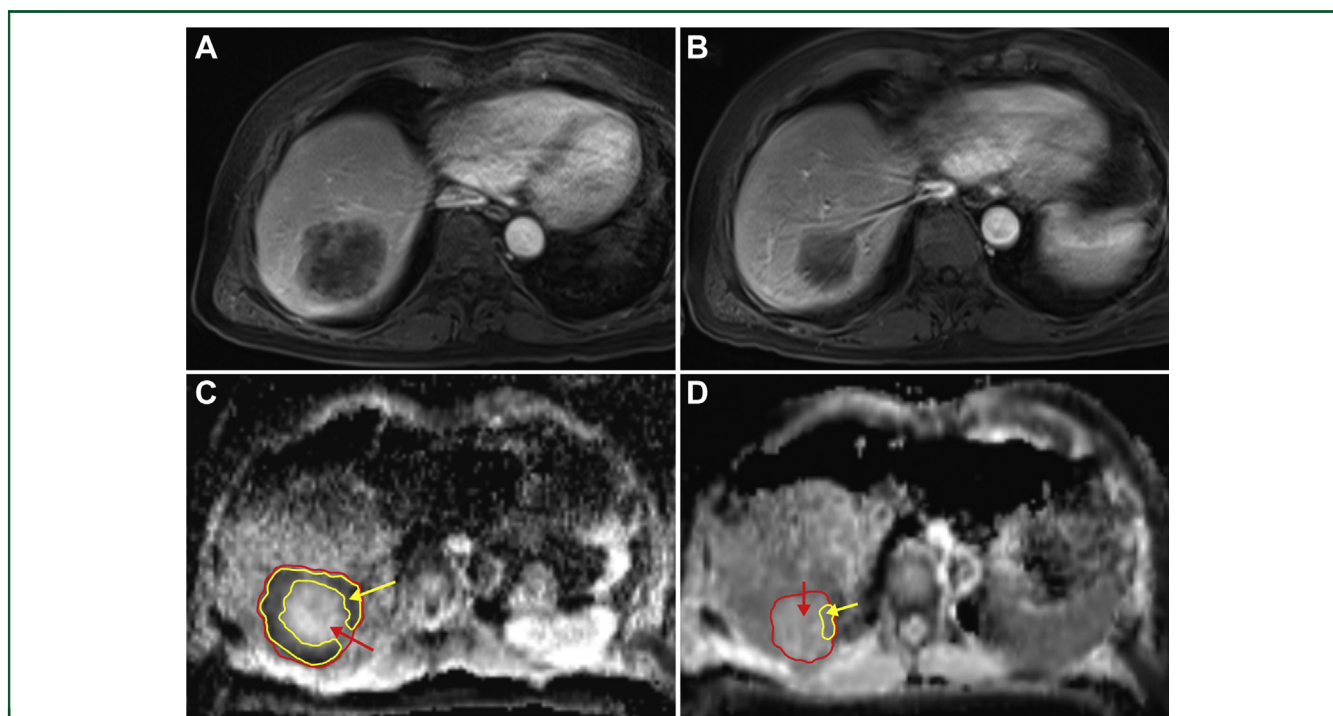


Figure 1. Contrast-enhanced magnetic resonance imaging (MRI) and diffusion-weighted imaging. A gadolinium-enhanced T1 volumetric interpolated breath-hold examination (VIBE) MRI of a liver metastasis before (A) and after (B) chemotherapy. The corresponding apparent diffusion coefficient (ADC) maps calculated from diffusion-weighted images (DWI) of the same tumour before (C) and after systemic therapy (D). Red area and arrow: whole tumour area. Yellow area and arrow: the postulated active tumour area (ADC periphery, the C-formed rim in image C).

somewhat longer than the regular protocol of 40 min. A navigator belt was used to trigger ^1H -MRS and DWI acquisitions to the end of exhalation. The exact sequences are listed in [Supplementary Table S1](https://doi.org/10.1016/j.esmooop.2021.100208), available at <https://doi.org/10.1016/j.esmooop.2021.100208>.

DWI and ^1H -MRS data evaluation

DWI and ^1H -MRS data were analysed independently of the clinical data by a physicist specialised in MRI physics blinded to other clinical data (AIH). The ADC maps were calculated from DWI by using the largest area in the axial plane of the largest liver metastasis and drawing the boundaries of the region of interest (ROI) within the metastasis. The ADC maps were calculated for both the whole metastasis area and for the peripheral part with lowest ADC values. This peripheral lowest ADC part is assumed to present the most cellular area of the tumour. The mean ADC value for ROI (ADC) was used. The measurements were carried out for the same metastasis both before and after systemic therapy ([Figure 1](https://doi.org/10.1016/j.esmooop.2021.100208)). ^1H -MR spectra were analysed with LCModel v6.3 software (<http://lcmode.ca/lcmode.shtml>) to assess the amount of free choline-containing compounds (CCC) in the metastasis and fat accumulation in the liver parenchyma outside the tumour.^{23,24} For assessment of hepatocellular lipids, intensities of methylene and water resonances were determined, and liver fat content was calculated as described previously.²⁵ Concentration of CCC was determined from water-suppressed spectra using an unsuppressed water signal as a concentration reference in the LCModel. ^1H -MRS measurements were done before and

after treatment ([Supplementary Figure S1](https://doi.org/10.1016/j.esmooop.2021.100208), available at <https://doi.org/10.1016/j.esmooop.2021.100208>).

CE-MRI evaluation

The MRI was initially evaluated for clinical use by the local radiologists at the university hospitals. A radiologist specialised in liver imaging (AO) re-evaluated the MRIs with RECIST 1.1 criteria and measured the change of largest axial plane area and diameter, and as an experimental endpoint with morphologic criteria adapted to MRI from CT criteria described by Chun et al.¹⁶ In short, the MRI morphologic response was evaluated using a semi-quantitative three-step scale. A metastasis with heterogeneous attenuation and a thick, poorly defined tumour–liver interface or a peripheral rim of hyperattenuating contrast enhancement was placed in the group 3. A metastasis with homogeneous attenuation with a thin, sharply defined tumour–liver interface or resolution of the enhancing tumour rim belonged to the group 1. The metastases between these two formed the group 2. A change from group 2 or 3 to 1 was considered as optimal response and from 3 to 2 as partial response. This evaluation was done independently from clinical data.

Histological evaluation

A gastrointestinal pathologist (AR) re-evaluated the histological slides from liver resection specimens independently from radiological and clinical data. A standardised liver resection pathology form was used ([Supplementary Table S2](https://doi.org/10.1016/j.esmooop.2021.100208), available at <https://doi.org/10.1016/j.esmooop.2021.100208>). Haematoxylin–eosin, Herovici and periodic

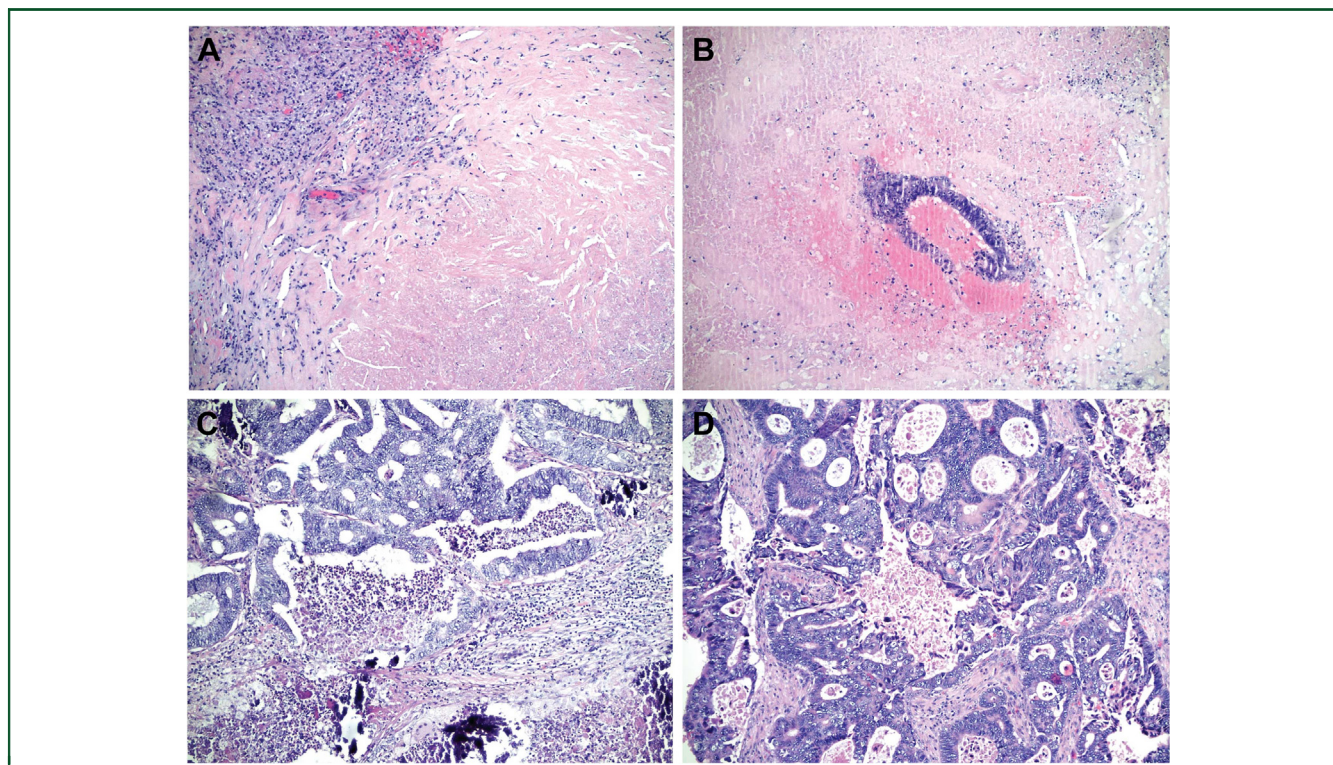


Figure 2. Tumour vitality (TV), tumour regression grade (TRG) and modified tumour regression grade (mTRG) after neoadjuvant or conversion therapy.

(A) No vital tumour cells, fibrosis and infarct-like necrosis, TV 0%, TRG1, mTRG1. (B) A small area of vital tumour cells surrounded by large areas of relatively clean (infarct-like) necrosis, TV 10%, TRG2, mTRG2. (C) Larger areas of vital tumour cells bordered by vital stroma and areas of 'dirty' (usual) necrosis, with infarct-like necrosis elsewhere in the slide (not shown), TV 30%, TRG3, mTRG3. (D) Mostly vital tumour, with little fibrosis and necrosis, TV 70%, TRG4, mTRG4.

acid–Schiff stains were used. Tumour diameter was measured from the original resection block. Tumour vitality was defined as the ratio of vital tumour cells to whole tumour and presented as percent. The tumour histology was further evaluated using tumour regression grade (TRG) and further histological response categories described by Rubbia-Brandt et al.²⁶ and by defining distinct types of necrosis: usual necrosis associated with uncontrolled tumour growth and infarct-like necrosis associated with response to chemotherapy (Figure 2).^{27,28} A modified tumour regression grade (mTRG) was formed by combining TRG with necrosis data.²⁷

Chemotherapy regimens

Standard local treatment protocols based on European Society for Medical Oncology⁶ and National Comprehensive Cancer Network^{7,8} guidelines were used in the neoadjuvant or conversion chemotherapy (NAC), until disease progression, toxicity or resectability was achieved. In the neoadjuvant setting, oxaliplatin and fluoropyrimidine-based treatment was used,²⁹ and in the conversion setting, the most intensive tolerable regimen was used, mostly a doublet or triplet chemotherapy combined with a targeted agent (bevacizumab, cetuximab or panitumumab) based on *RAS* and *BRAF* status.⁶ Bevacizumab treatment was stopped 5–6 weeks before liver resection and one further cycle of chemotherapy was given, as appropriate.

Statistical analysis

Statistical analyses were carried out using IBM SPSS Statistics version 25 software (IBM Corp., Armonk, NY). Continuous variables with non-normal distribution are presented as median with range, independent samples compared using Mann–Whitney *U* test and related samples using Wilcoxon signed rank test. Categorical variables are presented as absolute numbers (percentage) and compared using chi-square or Fisher's exact test, as appropriate. Risk ratios (RRs) and 95% confidence intervals (95% CI) were calculated to identify the association between ADC (e.g. ADC < 1.20 versus ADC ≥ 1.20) and response variables, and between chemotherapy (NAC + targeted versus NAC no targeted) and response variables. Due to small sample size, the exact methods were applied for CI and for testing the RRs. For response variables with zero cell counts, the zero-count adjustment was done by adding 0.50 to zero cell counts. The RR analyses were carried out using NCSS Statistical Software (2019), LLC (Kaysville, UT). Correlation analysis was compared using Spearman's rho. Follow-up time was calculated using reverse Kaplan–Meier curves. Survival was estimated using Kaplan–Meier curves and analysed by log-rank and Cox regression methods. OS was calculated from the date of diagnosis of mCRC to the date of death from any cause, or censored at last follow-up. Progression-free survival (PFS) was calculated from mCRC diagnosis to relapse after resection/local ablative therapy, progression, death from any cause or censored at follow-up.

Table 1. Baseline demographics			
	All n (%)	Liver resection n (%)	Systemic therapy only n (%)
	52 (100)	40 (77)	12 (23)
Median age (range), years	64.5 (41-80)	62.5 (41-80)	68 (56-77)
Female sex	22 (42)	18 (45)	4 (33)
Male sex	30 (58)	22 (55)	8 (67)
ECOG PS 0	16 (3)	15 (38)	1 (8)
ECOG PS 1	31 (60)	24 (60)	7 (58)
ECOG PS 2	5 (10)	1 (3)	4 (33)
Charlson Comorbidity Index, median (range)	8 (6-13)	8 (6-13)	9 (8-10)
Synchronous metastases	33 (63)	26 (65)	7 (58)
Early metachronous metastases ^a	7 (13)	4 (10)	3 (25)
Late metachronous metastases ^a	12 (23)	10 (25)	2 (17)
Primary in right colon	12 (23)	9 (23)	3 (25)
Primary in left colon	22 (42)	20 (50)	2 (17)
Primary in rectum	18 (35)	11 (28)	7 (58)
Node positive primary	39 (75)	29 (73)	10 (83)
Grade 1	7 (1)	6 (15)	1 (8)
Grade 2	36 (69)	30 (75)	6 (50)
Grade 3	3 (6)	2 (5)	1 (8)
Grade unknown	6 (12)	2 (5)	4 (33)
KRAS mutation	17 (33)	14 (35)	3 (25)
NRAS mutation of tested ^b	1 (2)	1/32 (3)	0/9 (0)
BRAF mutation of tested ^b	7 (13)	3/32 (9)	4/11 (36)
One liver metastasis	20 (38)	16 (40)	4 (33)
Two liver metastases	14 (27)	12 (30)	2 (17)
Three or more liver metastases	18 (35)	12 (30)	6 (50)
Chemotherapy treatment	47 (94)	35 (88)	12 (100)
VEGF antibodies	21 (40)	18 (45)	3 (25)
EGFR antibodies	7 (14)	5 (13)	2 (17)
Time from last MRI to operation in days, median (range)		43 (2-232)	
Elevated CEA at MRI1	36/51 (71)	25/39 (64)	11/12 (92)
Elevated CEA at MRI2	12/38 (32)	5/27 (19)	7/11 (64)
Elevated CEA at operation		8/39 (21)	
Elevated CA19-9 at MRI1	18/38 (47)	14/31 (45)	4/7 (57)
Elevated CA19-9 at MRI2	14/27 (52)	9/20 (45)	5/7 (71)
Elevated CA19-9 at operation		6/20 (30)	

CA19-9, carbohydrate antigen 19-9; CEA, carcinoembryonic antigen; ECOG PS, Eastern Cooperative Oncology Group performance status; EGFR, endothelial growth factor receptor; VEGF, vascular endothelial growth factor.

^a Early metachronous from diagnosis to 12 months and late metachronous >12 months from colorectal cancer diagnosis.

^b NRAS mutation analysed in 41/52, BRAF mutation analysed in 43/52.

Two-tailed *P* values <0.05 were considered statistically significant. Receiver operating characteristic analyses were carried out to determine whether mean would be a suitable cut-off for ADC (Supplementary Table S3, available at <https://doi.org/10.1016/j.esmoop.2021.100208>).

RESULTS

Fifty-two eligible patients had at least one MRI with DWI and ¹H-MRS (flow chart in Supplementary Figure S1, available at <https://doi.org/10.1016/j.esmoop.2021.100208>). Thirty-nine patients had MRI both at baseline and first response evaluation after 2-3 months of first-line therapy. Reverse median Kaplan–Meier follow-up was 65 (95% CI 34-95) months. Demographics are presented in Table 1. Forty patients (77%) had liver resection, of which 37 with complete resection, and 37 had received NAC. Forty-seven received NAC, of which 12 could not be converted and received systemic therapy alone. Partial response on NAC according to RECIST was seen in 51% and stable disease in 49% (Table 2). An optimal morphologic MRI response of the largest lesion was noted in 32%, partial response in 26% and no response in 42%, with

corresponding 5-year OS rates of 46%, 51% and 22%, respectively (*P* = 0.092). Median time interval between MRI assessments was 65 days (range 37-174 days) and between the last MRI and operation was 44 days (range 2-234 days).

Five patients (13%) had a pathologic complete response, i.e. vitality 0%, TRG1 and mTRG1 (Table 2). A major response to NAC (1%-10% vitality) was seen in 46%, with TG1-2 in 40% and with mTRG1-2 (including necrosis) in 46%.

Baseline ADC

A baseline ADC measurement of the largest metastasis was available in 40 patients with a median value of 1.20×10^{-3} mm²/s. A baseline ADC value <1.20 (below median) versus ≥1.20 was associated with partial response on MRI according to RECIST criteria (85% versus 30%; RR 0.22; Table 2). Non-significant inverse trends for associations with baseline ADC values were noted for morphologic responses on MRI, tumour vitality, TRG, mTRG (Table 2) or conversion to resectable. No significant associations with OS or PFS were seen (Supplementary Table S4, available at <https://doi.org/10.1016/j.esmoop.2021.100208>).

Table 2. Association between ADC at baseline, at response evaluation and change in ADC with NAC versus RECIST and morphologic response criteria, tumour vitality, TRG and mTRG

	All NAC	Baseline ADC			Response ADC			Change ADC with NAC		
		ADC < 1.20	ADC ≥ 1.20	RR (95% CI) ^a	ADC < 1.29	ADC ≥ 1.29	RR (95% CI) ^b	Reduced	Not reduced	RR (95% CI) ^c
Radiology after chemotherapy, n (%)	39	13	20		17	18		10	22	
MRI RECIST criteria										
Partial response	20 (51)	11 (85)	6 (30)		13 (76)	5 (28)		6 (60)	11 (50)	
Stable disease	19 (49)	2 (15)	14 (70)	0.22 (0.05-0.65)	4 (24)	13 (72)	0.33 (0.13-0.74)	4 (40)	11 (50)	0.80 (0.33-1.75)
Morphologic MRI criteria ^d										
Optimal response	12 (32)	4 (31)	7 (35)		6 (35)	5 (28)		3 (30)	7 (32)	
Partial response	10 (26)	3 (23)	6 (30)		5 (29)	5 (28)		4 (40)	5 (23)	
No response	16 (42)	6 (46)	7 (35)	1.32 (0.55-3.04)	6 (35)	8 (44)	0.79 (0.34-1.79)	3 (30)	10 (45)	1.52 (0.53-4.34)
Histology after chemotherapy, n (%)	35	13	14		13	11		7	15	
Tumour vitality										
0	5 (17)	4 (31)	1 (7)		4 (31)	1 (9)		1 (14)	4 (27)	
1-30	16 (53)	4 (31)	10 (71)		5 (38)	7 (64)		4 (57)	7 (47)	
31-100	9 (30)	5 (38)	3 (21)	1.79 (0.57-5.95) ^e	4 (31)	3 (27)	1.13 (0.36-3.77) ^e	2 (29)	4 (27)	1.07 (0.24-3.84) ^e
TRG										
1-2	14 (40)	6 (46)	7 (50)		5 (38)	5 (45)		3 (43)	7 (47)	
3	12 (34)	3 (23)	5 (36)		4 (31)	6 (55)		2 (29)	6 (40)	
4-5	9 (26)	4 (31)	2 (14)	2.15 (0.55-9.87) ^f	4 (31)	0 (0)	7.08 (0.78-77.6) ^f	2 (29)	2 (13)	2.14 (0.37-12.10) ^f
mTRG										
1-2	16 (46)	7 (54)	7 (50)		6 (46)	6 (55)		3 (43)	8 (53)	
3	12 (34)	3 (23)	6 (43)		4 (31)	5 (45)		3 (43)	5 (33)	
4-5	7 (20)	3 (23)	1 (7)	3.23 (0.51-38.0) ^f	3 (23)	0 (0)	5.31 (0.65-60.2) ^f	1 (14)	2 (13)	1.07 (0.08-7.17) ^f

ADC, apparent diffusion coefficient; CI, confidence interval; MRI, magnetic resonance imaging; mTRG, modified tumour regression grade; NAC, neoadjuvant or conversion chemotherapy; RR, risk ratio; TRG, tumour regression grade.

^a RR = Occurrence of outcome if median ADC <1.20/occurrence of outcome if median ADC ≥1.20.

^b RR = Occurrence of outcome if median ADC <1.29/occurrence of outcome if median ADC ≥1.29.

^c RR = Occurrence of outcome if ADC reduced with NAC, i.e. decreasing/occurrence of outcome if ADC not reduced, i.e. same or increasing with NAC.

^d MRI was not diagnostic for morphology because of motion artefact.

^e Comparison groups for RR vitality 0%-30% versus 31%-100%.

^f Comparison groups for RR TRG and mTRG 1-3 versus 4-5.

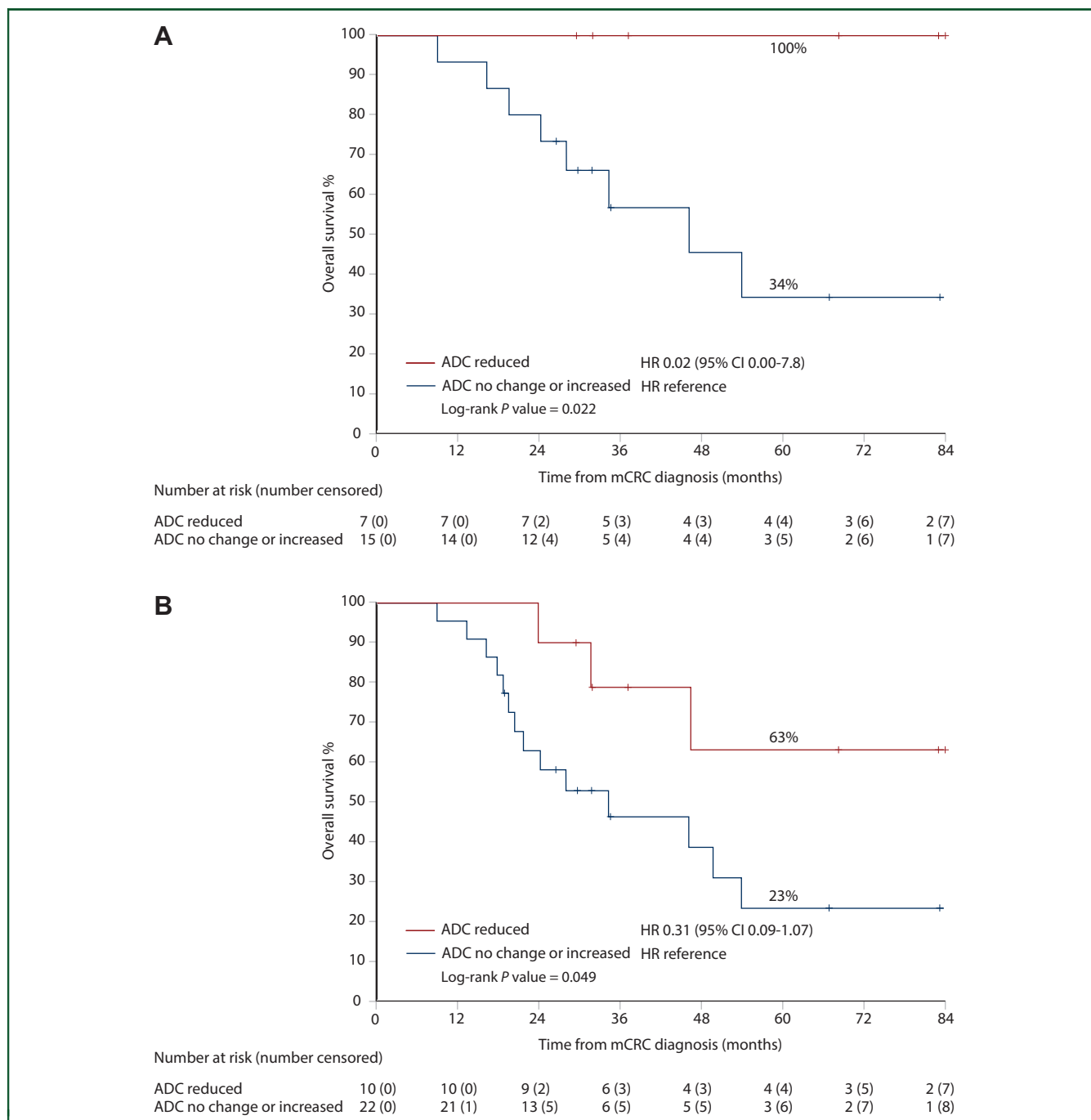


Figure 3. Overall survival in patients whose liver metastases show a reduction versus increase or no change in the ADC after chemotherapy.

(A) Resected patients. (B) All patients treated with neoadjuvant or conversion therapy.

ADC, apparent diffusion coefficient; CI, confidence interval; HR, hazard ratio; mCRC, metastatic colorectal cancer.

The baseline ADC maps for the peripheral lowest ADC value areas within the metastasis (ADC periphery) had a median of $0.92 \times 10^{-3} \text{ mm}^2/\text{s}$, and <0.92 versus ≥ 0.92 showed no significant associations with RECIST criteria, MRI morphology, metastasis vitality, TRG, mTRG, PFS or OS (Supplementary Tables S4 and S5, available at <https://doi.org/10.1016/j.esmoop.2021.100208>).

Response evaluation ADC

After NAC, median ADC at response evaluation was $1.29 \times 10^{-3} \text{ mm}^2/\text{s}$ in the whole metastasis. ADC <1.29 (under

median) versus ≥ 1.29 was associated significantly with partial response according to RECIST (RR 0.33, Table 2), but was not associated with morphologic MRI criteria or vitality. Response ADC <1.29 showed non-significant inverse trends for association with TRG and mTRG.

After NAC, the median ADC periphery was $1.13 \times 10^{-3} \text{ mm}^2/\text{s}$. A reduction of ADC periphery from baseline was associated with partial response (RR 0.40) and showed non-significant inverse trends for TRG and mTRG. No associations with OS or PFS were noted (Supplementary Tables S4 and S5, available at <https://doi.org/10.1016/j.esmoop.2021.100208>).

Change in ADC with NAC

A decrease in ADC values (4%-93% decrease from baseline to after NAC) was seen in 10 patients (31%), and showed no association with RECIST, morphologic MRI, tumour vitality, TRG or mTRG (Table 2). TRG and mTRG showed non-significant inverse associations for reduced ADC periphery (Supplementary Table S5, available at <https://doi.org/10.1016/j.esmoop.2021.100208>). Change in ADC showed no association with fibrosis ($P = 1.00$) or steatosis ($P = 1.00$) in histology.

Patients with a decrease in the ADC values had better OS than patients with an increase or no change in ADC (Supplementary Table S4, available at <https://doi.org/10.1016/j.esmoop.2021.100208>, Figure 3). In patients with liver resection, a decrease in ADC versus increase or no change were associated with 5-year OS rates of 100% and 34%, respectively ($P = 0.022$, Figure 3A). An OS advantage for decreased ADC was seen also in patients receiving NAC with/without resection, with 5-year OS rates of 63% versus 23%, respectively ($P = 0.049$, Figure 3B). An OS advantage for decreased ADC was seen in patients receiving NAC with targeted agents ($n = 6$ decreased ADC versus 13 increased or no change, $P = 0.029$). A decrease in ADC periphery values versus increased or no change did not show a difference in OS (Supplementary Table S4, available at <https://doi.org/10.1016/j.esmoop.2021.100208>).

Response evaluation ADC under a median of 1.29 was associated with better 3-year PFS (42% versus 17%), but no other significant differences in PFS between groups were noted (Supplementary Table S4, available at <https://doi.org/10.1016/j.esmoop.2021.100208>).

A decrease in the ADC after NAC showed no statistical difference in DFS after resection ($n = 6$ decreased versus 13 increased or no change), with 5-year DFS rates of 67% versus 45%, respectively ($P = 0.273$).

NAC with or without targeted agents

Targeted agents with VEGF antibodies (bevacizumab, $n = 21$), EGFR antibodies (cetuximab or panitumumab, $n = 8$), both ($n = 1$) and combination chemotherapy only ($n = 6$) were given. ADC decrease did not show any significant differences for chemotherapy with targeted agents or without. Responders versus non-responders had no significant difference in fibrosis ($P = 0.47$) or steatosis ($P = 0.57$) in histology.

Patients receiving NAC including targeted agents had a higher likelihood of having low tumour vitality 0%-10% (RR 7.17, 95% CI 1.12-66), mTRG1-2 (RR 7.17, 95% CI 1.12-66) and a trend for TRG1-2 (RR 6.28, 95% CI 0.96-58), when compared to patients receiving chemotherapy alone.

Survival, MRI response and histology

Tumour vitality, TRG or mTRG were not significantly associated with OS or PFS (Supplementary Table S4, available at <https://doi.org/10.1016/j.esmoop.2021.100208>). Response on MRI according to RECIST or morphologic criteria was not significantly associated with tumour vitality, TRG or mTRG

(Supplementary Table S6, available at <https://doi.org/10.1016/j.esmoop.2021.100208>).

¹H-MRS

A ¹H-MRS was evaluated in 21 patients, of which 14 were operated after NAC. Although decreases in choline levels in ¹H-MRS seemed to reflect response to NAC in some patients (Supplementary Figure S2, available at <https://doi.org/10.1016/j.esmoop.2021.100208>), no significant associations were detected between the baseline relative amounts of free choline versus response on RECIST, morphologic MRI criteria, tumour vitality, TRG or mTRG after NAC. Seven patients had a second ¹H-MRS after NAC, with a decrease in free choline in four with partial response in RECIST, without statistical significance.

The ¹H-MRS estimation of liver adiposity, i.e. accumulation of fat in the liver, in the MRI after NAC was associated with macrovesicular steatosis in histological evaluation of the liver resection specimens ($n = 20$, $P < 0.001$, R^2 linear = 0.666 when MRI was done within 60 days before liver surgery, Supplementary Figure S3, available at <https://doi.org/10.1016/j.esmoop.2021.100208>). According to ¹H-MRS analysis, liver steatosis increased in 86% of patients during NAC ($n = 21$, $P = 0.001$).

DISCUSSION

In this prospective study of CRC patients with liver metastases, we analysed systemic treatment-induced morphologic and metabolic changes in CE-MRI, including ADC values of DWI-MRI and ¹H-MRS, in comparison with histology of resected liver metastases as 'gold standard' and in relation to survival.

Patients with a baseline ADC below median had better treatment responses according to RECIST in the present study. This is in line with earlier studies comparing RECIST or similar size-based criteria.^{11,30-33} There is no significant association of ADC and morphologic MRI criteria for response, and to our knowledge this has not been studied before. Lower ADC represents higher cellularity and thus possibly a more responding lesion.^{11,12} Low pre-treatment ADC was not statistically associated with OS or PFS in our study, in line with findings by Tam et al.,³⁴ but contrary to the study by Heijmen et al., where low baseline ADC was associated with shorter OS and PFS in patients receiving chemotherapy.³⁵ Baseline low ADC is counterintuitive for shorter OS and PFS, as low ADC has consequently shown association with better responses,^{11,30-33} a strong positive predictor for better PFS and OS.¹⁴

Low ADC values after NAC also indicated better treatment response according to RECIST, but not according to morphologic MRI criteria. This is in line with previous findings in rectal primaries treated with chemotherapy,³⁶ but there low ADC in responders after 10-12 weeks of chemotherapy was considered loss of non-viable fraction of the treated tumour. Non-responders had high ADC after chemotherapy.³⁶ Low ADC could also represent increased fibrosis or steatosis in the tumour tissue due to treatment

response at 10-12 weeks, when tumour cells have been replaced with collagen, and thus low motility of water molecules. Low ADC values have been shown in liver cirrhosis, i.e. fibrous tissue with high collagen content.³⁷ We noted an improved PFS for patients with low ADC at response evaluation. This inverse correlation between ADC and treatment response and outcome is rarely reported in other studies.

ADC change did not significantly associate with response according to RECIST after a median of 9 weeks of NAC. In early evaluation time point, two studies are in line with our findings (1-2 weeks between imaging),^{35,38} whereas two studies show that an elevation in ADC during chemotherapy predicts better response (0.5-2 weeks' imaging interval).^{30,39} Increase in ADC at an early evaluation time point probably measures changes in cellularity and possibly inflammation. Later response evaluation of liver metastases (after 9-15 weeks), as in our study, has been evaluated in one prior small study ($n = 20$).¹¹ The findings at baseline are in line, as low baseline ADC correlates with better response, but change was contrary to our findings, as increasing ADC was associated with better treatment response.¹¹ The rectal cancer study is contrary to both our and Koh et al.'s studies, as a decreasing ADC is linked to better chemotherapy response.³⁶ Low response ADC or decreasing ADC during chemotherapy could theoretically be linked to increasing fibrosis or steatosis in treatment response, but this could not be histologically verified in our small subgroup analyses.

Decreasing ADC associates with better OS in our study, both in resected and in patients receiving systemic therapy with/without targeted agents. Contrary to the present study, two studies report that ADC change was not predictive for OS with 1-week³⁵ or 12-week imaging intervals.³⁴ In line with these findings, even though the patients with low response ADC had longer PFS, we found no significant difference in PFS whether ADC decreased with systemic therapy or not.

Only a few studies using histology as a reference for ADC behaviour after preoperative systemic therapy are available. Low ADC values are thought to present vital tumour area.³⁰ Chiaradia et al.⁴⁰ show that high ADC correlates with tumour necrosis after chemotherapy, but generally not with tumour vitality because of varying amounts of fibrosis and scattered distribution of tumour cells, this is in line with the non-significant trends for TRG and mTRG in our study. Some correlation with ADC and vitality has been noted in patients treated with targeted agents.⁴⁰ Donati et al.⁴¹ reported that high ADC of the whole tumour or tumour periphery after NAC correlates inversely with low tumour vitality and TRG1-2. Wagner et al.⁴² found no association between whole metastasis ADC and histology after NAC, but ADC of the periphery was higher for metastases with major histological response. A study by Dunet et al.⁴³ shows that positron emission tomography findings after NAC correlate with TRG, but do not associate with ADC. These earlier studies comparing ADC with histology reported only MRI findings

after NAC and thus the importance of changes in ADC could not be compared. An elevation in ADC value is thought to present a higher degree of freedom of water molecules in the tissue, which could be due to increased necrosis and reduced cellularity.⁴⁴ Our study shows only non-significant inverse trends in histological associations with changes in ADC during NAC versus tumour necrosis, e.g. tumour vitality, TRG or mTRG. Response by RECIST or morphologic criteria did not capture responses in histology, neither with vitality, TRG or mTRG in this population. Histology, on the other hand, did not associate with OS or PFS either. ¹H-MRS can be used to analyse the amount of free choline and other CCCs and it is usually clearly higher in the liver metastasis than in the surrounding liver parenchyma,^{23,45} but it has not widely been studied in this setting. In our study, no association was detected between the relative amounts of free choline in the largest metastasis at baseline versus response according to RECIST or morphologic MRI criteria, neither in histological findings. Future studies are needed to evaluate its role in detecting treatment efficacy.

The use of ¹H-MRS in detecting hepatic steatosis is better described,²⁴ and the present study agrees with earlier reports where ¹H-MRS evaluation of liver adiposity correlates well with histology.⁴⁶ Patients also seem to acquire fat in their livers during NAC, which is a known side-effect of chemotherapy agents.⁴⁷

The strength of this study lies in its prospective multi-centre design with repeated assessment, standardised MRI methodology and uniform radiological and histological re-evaluation at a highly specialised tertiary liver centre. Identification of patients was challenging as eligibility was to be checked by oncologist, radiologist and physicist at the time of referral before first appointment at oncology, as postponing treatment due to study procedures was not acceptable. This substudy also needed excellent MRI facilities which were available only in four university hospitals. To our knowledge, this small series is still the largest prospective, multicentre study of repeated DWI with histological correlation, combined with comprehensive survival data of patients treated with chemotherapy and/or resection. The small subgroups due to the prospective nature of the study and technical challenges, especially with repeated DWI and ¹H-MRS, make the present findings hypothesis generating. A further limitation is that we analysed only the largest lesion and heterogeneity between metastases seen in one-fifth of metastases,⁴⁸ which thus was possibly missed. The ongoing DREAM study (NCT02781935) would, if completed, be the largest study to evaluate MR DWI in detecting chemotherapy response of colorectal liver metastases.

Conclusions

Liver metastases respond to chemotherapy and targeted agents not only by shrinking in size but also by changes in morphology and metabolic activity, which associates

with survival. Conventional imaging modalities might be insufficient in detecting treatment response and MR DWI, especially low or decreasing ADC, provides additional information also for survival, but do not associate significantly with histological findings.

ACKNOWLEDGEMENTS

The authors wish to thank all the collaborators of this study, in particular the study nurses at the participating hospitals and statistician Tuija Poussa for providing help with statistical analyses.

The RAXO Study Group Collaborators: Heikki Mäkisalo, Riikka Huuhtanen, Juhani Kosunen, Sirpa Leppä, Petri Bono, Johanna Mattson, Emerik Österlund, Heidi Penttinen, Siru Mäkelä, Olli Carpén, Marjut Timonen, Kaisa Lehtomäki, Veera Salminen, Niina Paunu, Martine Vornanen, Nieminen Lasse, Eetu Heervä, Eija Korkeila, Eija Sutinen, Maija Lavonius, Jari Sundström, Markus Mäkinen, Tuija Poussa.

FUNDING

This investigator-initiated RAXO study was supported by Finska Läkaresällskapet (2015, 2016, 2017, 2018, 2019, 2020, 2021); Cancer Foundation Finland (2018-2019, 2020); Relander's Foundation (2020-2022); the Competitive State Research Financing of the Expert Responsibility Area of Tampere, Helsinki and Turku (2016, 2017, 2018, 2019, 2020, 2021); Tampere University Hospital Funds (Tukisäätiö 2019, 2020; OOO 2020); and the Research Fund of Helsinki University Hospital (2019, 2020). The infrastructure with database and study nurses were partly supported by pharmaceutical companies (Amgen—unrestricted grant 2012-2020, Lilly 2012-2017, Merck KGaA 2012-2020, Roche Finland 2012-2020, Sanofi 2012-2017 and Servier—unrestricted grant 2016-2020). The funders had no role in the study design, analysis, interpretation of the data, decision to publish or writing of this report. All authors had full access to the data and had final responsibility for the decision to submit for publication.

DISCLOSURE

AU, AIH, AO, AR, NL, RK, L-MS, TKS, PMH, RHR, AN, RBS, IR-K, EL, JV, EP, PO, AÅ, EL, JS, PR, EL and HMI have received travel grants and/or honoraria from the following pharmaceutical companies: Amgen, Bayer, BMS, Celgene, Erytech Pharma, Janssen-Cilag, Lilly, Merck, MSD, Nordic Drugs, Roche, Sanofi, Servier/Shire, Sobri, Pierre Fabre and Varian.

REFERENCES

- Hackl C, Neumann P, Gerken M, Loss M, Klinkhammer-Schalke M, Schlitt HJ. Treatment of colorectal liver metastases in Germany: a ten-year population-based analysis of 5772 cases of primary colorectal adenocarcinoma. *BMC Cancer*. 2014;14:810.
- Vayrynen V, Wirta EV, Seppala T, et al. Incidence and management of patients with colorectal cancer and synchronous and metachronous colorectal metastases: a population-based study. *BJS Open*. 2020;4(4):685-692.
- Scherman P, Syk I, Holmberg E, Naredi P, Rizell M. Influence of primary tumour and patient factors on survival in patients undergoing curative resection and treatment for liver metastases from colorectal cancer. *BJS Open*. 2020;4(1):118-132.
- Adam R, Kitano Y. Multidisciplinary approach of liver metastases from colorectal cancer. *Ann Gastroenterol Surg*. 2019;3(1):50-56.
- Lam VW, Spiro C, Laurence JM, et al. A systematic review of clinical response and survival outcomes of downsizing systemic chemotherapy and rescue liver surgery in patients with initially unresectable colorectal liver metastases. *Ann Surg Oncol*. 2012;19(4):1292-1301.
- Van Cutsem E, Cervantes A, Adam R, et al. ESMO consensus guidelines for the management of patients with metastatic colorectal cancer. *Ann Oncol*. 2016;27(8):1386-1422.
- Benson A, Venook A. *NCCN Guidelines for Colon Cancer*. National Comprehensive Cancer Network. 2020. Available at https://www.nccn.org/professionals/physician_gls/pdf/colon.pdf. Accessed February 17, 2020.
- Benson AB, Venook A. *NCCN Guidelines for Rectal Cancer*. National Comprehensive Cancer Network. 2020. Available at https://www.nccn.org/professionals/physician_gls/pdf/rectal.pdf. Accessed February 17, 2020.
- Weledji EP. Centralization of liver cancer surgery and impact on multidisciplinary teams working on stage IV colorectal cancer. *Oncol Rev*. 2017;11(2):331.
- Fraum TJ, Owen JW, Fowler KJ. Beyond histologic staging: emerging imaging strategies in colorectal cancer with special focus on magnetic resonance imaging. *Clin Colon Rectal Surg*. 2016;29(3):205-215.
- Koh DM, Scurr E, Collins D, et al. Predicting response of colorectal hepatic metastasis: value of pretreatment apparent diffusion coefficients. *AJR Am J Roentgenol*. 2007;188(4):1001-1008.
- Luna A, Pahwa S, Bonini C, Alcalá-Mata L, Wright KL, Gulani V. Multi-parametric MR imaging in abdominal malignancies. *Magn Reson Imaging Clin N Am*. 2016;24(1):157-186.
- Lewis S, Dyvorne H, Cui Y, Taouli B. Diffusion-weighted imaging of the liver: techniques and applications. *Magn Reson Imaging Clin N Am*. 2014;22(3):373-395.
- Eisenhauer EA, Therasse P, Bogaerts J, et al. New response evaluation criteria in solid tumours: revised RECIST guideline (version 1.1). *Eur J Cancer*. 2009;45(2):228-247.
- Schwartz LH, Litiere S, de Vries E, et al. RECIST 1.1-update and clarification: from the RECIST committee. *Eur J Cancer*. 2016;62:132-137.
- Chun YS, Vauthey JN, Boonsirikamchai P, et al. Association of computed tomography morphologic criteria with pathologic response and survival in patients treated with bevacizumab for colorectal liver metastases. *J Am Med Assoc*. 2009;302(21):2338-2344.
- Hirashima Y, Yamada Y, Tateishi U, et al. Pharmacokinetic parameters from 3-Tesla DCE-MRI as surrogate biomarkers of antitumor effects of bevacizumab plus FOLFIRI in colorectal cancer with liver metastasis. *Int J Cancer*. 2012;130(10):2359-2365.
- Anzidei M, Napoli A, Zaccagna F, et al. Liver metastases from colorectal cancer treated with conventional and antiangiogenic chemotherapy: evaluation with liver computed tomography perfusion and magnetic resonance diffusion-weighted imaging. *J Comput Assist Tomogr*. 2011;35(6):690-696.
- De Bruyne S, Van Damme N, Smeets P, et al. Value of DCE-MRI and FDG-PET/CT in the prediction of response to preoperative chemotherapy with bevacizumab for colorectal liver metastases. *Br J Cancer*. 2012;106(12):1926-1933.
- Karlas T, Petroff D, Garnov N, et al. Non-invasive assessment of hepatic steatosis in patients with NAFLD using controlled attenuation parameter and 1H-MR spectroscopy. *PLoS One*. 2014;9(3):e91987.
- Osterlund P, Salminen T, Soveri LM, et al. Repeated centralized multidisciplinary team assessment of resectability, clinical behavior, and outcomes in 1086 Finnish metastatic colorectal cancer patients (RAXO): a nationwide prospective intervention study. *Lancet Reg Health Eur*. 2021;3:100049. <https://doi.org/10.1016/j.lanepe.2021.100049>.
- Isoniemi H, Uutela A, Nordin A, et al. Centralized repeated resectability assessment of patients with colorectal liver metastases during first-line

- treatment: prospective study. *Br J Surg*. 2021. <https://doi.org/10.1093/bjs/znaa145>.
23. Fischbach F, Schirmer T, Thormann M, Freund T, Ricke J, Bruhn H. Quantitative proton magnetic resonance spectroscopy of the normal liver and malignant hepatic lesions at 3.0 Tesla. *Eur Radiol*. 2008;18(11):2549-2558.
 24. Reeder SB, Cruite I, Hamilton G, Sirlin CB. Quantitative assessment of liver fat with magnetic resonance imaging and spectroscopy. *J Magn Reson Imaging*. 2011;34(4):729-749.
 25. Kotronen A, Peltonen M, Hakkarainen A, et al. Prediction of non-alcoholic fatty liver disease and liver fat using metabolic and genetic factors. *Gastroenterology*. 2009;137(3):865-872.
 26. Rubbia-Brandt L, Giostra E, Brezault C, et al. Importance of histological tumor response assessment in predicting the outcome in patients with colorectal liver metastases treated with neo-adjuvant chemotherapy followed by liver surgery. *Ann Oncol*. 2007;18(2):299-304.
 27. Chang HH, Leeper WR, Chan G, Quan D, Driman DK. Infarct-like necrosis: a distinct form of necrosis seen in colorectal carcinoma liver metastases treated with perioperative chemotherapy. *Am J Surg Pathol*. 2012;36(4):570-576.
 28. Ishida K, Uesugi N, Hasegawa Y, et al. Proposal for novel histological findings of colorectal liver metastases with preoperative chemotherapy. *Pathol Int*. 2015;65(7):367-373.
 29. Nordlinger B, Sorbye H, Glimelius B, et al. Perioperative FOLFOX4 chemotherapy and surgery versus surgery alone for resectable liver metastases from colorectal cancer (EORTC 40983): long-term results of a randomised, controlled, phase 3 trial. *Lancet Oncol*. 2013;14(12):1208-1215.
 30. Cui Y, Zhang XP, Sun YS, Tang L, Shen L. Apparent diffusion coefficient: potential imaging biomarker for prediction and early detection of response to chemotherapy in hepatic metastases. *Radiology*. 2008;248(3):894-900.
 31. Fouladi DF, Zarghampour M, Pandey P, et al. Baseline 3D-ADC outperforms 2D-ADC in predicting response to treatment in patients with colorectal liver metastases. *Eur Radiol*. 2020;30(1):291-300.
 32. Liang HY, Huang YQ, Yang ZX, et al. Potential of MR histogram analyses for prediction of response to chemotherapy in patients with colorectal hepatic metastases. *Eur Radiol*. 2016;26(7):2009-2018.
 33. Drewes R, Pech M, Powerski M, et al. Apparent diffusion coefficient can predict response to chemotherapy of liver metastases in colorectal cancer. *Acad Radiol*. 2020. <https://doi.org/10.1016/j.acra.2020.09.006>.
 34. Tam HH, Collins DJ, Brown G, et al. The role of pre-treatment diffusion-weighted MRI in predicting long-term outcome of colorectal liver metastasis. *Br J Radiol*. 2013;86(1030):20130281.
 35. Heijmen L, ter Voert EE, Oyen WJ, et al. Multimodality imaging to predict response to systemic treatment in patients with advanced colorectal cancer. *PLoS One*. 2015;10(4):e0120823.
 36. Dzik-Jurasz A, Domenig C, George M, et al. Diffusion MRI for prediction of response of rectal cancer to chemoradiation. *Lancet*. 2002;360(9329):307-308.
 37. Shin MK, Song JS, Hwang SB, Hwang HP, Kim YJ, Moon WS. Liver fibrosis assessment with diffusion-weighted imaging: value of liver apparent diffusion coefficient normalization using the spleen as a reference organ. *Diagnostics (Basel)*. 2019;9(3):107.
 38. Granata V, Fusco R, Catalano O, et al. Early assessment of colorectal cancer patients with liver metastases treated with antiangiogenic drugs: the role of intravoxel incoherent motion in diffusion-weighted imaging. *PLoS One*. 2015;10(11):e0142876.
 39. Kim JH, Joo I, Kim TY, Han S-W, Kim YJ, Lee JM, Han JK. Diffusion-related MRI parameters for assessing early treatment response of liver metastases to cytotoxic therapy in colorectal cancer. *AJR Am J Roentgenol*. 2016;207(3):W26-W32.
 40. Chiaradia M, Baranes L, Van Nhieu JT, et al. Intravoxel incoherent motion (IVIM) MR imaging of colorectal liver metastases: are we only looking at tumor necrosis? *J Magn Reson Imaging*. 2014;39(2):317-325.
 41. Donati F, Boraschi P, Pacciardi F, et al. 3T diffusion-weighted MRI in the response assessment of colorectal liver metastases after chemotherapy: correlation between ADC value and histological tumour regression grading. *Eur J Radiol*. 2017;91:57-65.
 42. Wagner M, Ronot M, Doblaz S, et al. Assessment of the residual tumour of colorectal liver metastases after chemotherapy: diffusion-weighted MR magnetic resonance imaging in the peripheral and entire tumour. *Eur Radiol*. 2016;26(1):206-215.
 43. Dunet V, Halkic N, Prior JO, et al. Detection and viability of colorectal liver metastases after neoadjuvant chemotherapy: a multiparametric PET/CT-MRI study. *Clin Nucl Med*. 2017;42(4):258-263.
 44. Granata V, Fusco R, Avallone A, et al. A radiologist's point of view in the presurgical and intraoperative setting of colorectal liver metastases. *Future Oncol*. 2018;14(21):2189-2206.
 45. Ter Voert E, Heijmen L, van Asten JJA, et al. Levels of choline-containing compounds in normal liver and liver metastases of colorectal cancer as recorded by (1) H MRS. *NMR Biomed*. 2019;32(1):e4035.
 46. Kim JW, Lee YS, Park YS, et al. Multiparametric MR index for the diagnosis of non-alcoholic steatohepatitis in patients with non-alcoholic fatty liver disease. *Sci Rep*. 2020;10(1):2671.
 47. Duwe G, Knitter S, Pesthy S, et al. Hepatotoxicity following systemic therapy for colorectal liver metastases and the impact of chemotherapy-associated liver injury on outcomes after curative liver resection. *Eur J Surg Oncol*. 2017;43(9):1668-1681.
 48. Sebagh M, Allard MA, Bosselut N, et al. Evidence of intermetastatic heterogeneity for pathological response and genetic mutations within colorectal liver metastases following preoperative chemotherapy. *Oncotarget*. 2016;7(16):21591-21600.